LETTERS

Dependence of single-molecule junction conductance on molecular conformation

Latha Venkataraman[1,4], Jennifer E. Klare[2,4], Colin Nuckolls[2,4], Mark S. Hybertsen[3,4] & Michael L. Steigerwald[2]

Since it was first suggested[1] that a single molecule might function as an active electronic component, a number of techniques have been developed to measure the charge transport properties of single molecules[2–12]. Although scanning tunnelling microscopy observations under high vacuum conditions can allow stable measurements of electron transport, most measurements of a single molecule bonded in a metal–molecule–metal junction exhibit relatively large variations in conductance. As a result, even simple predictions about how molecules behave in such junctions have still not been rigorously tested. For instance, it is well known[13,14] that the tunnelling current passing through a molecule depends on its conformation; but although some experiments have verified this effect[15–18], a comprehensive mapping of how junction conductance changes with molecular conformation is not yet available. In the simple case of a biphenyl—a molecule with two phenyl rings linked by a single C–C bond—conductance is expected to change with the relative twist angle between the two rings, with the planar conformation having the highest conductance. Here we use amine link groups to form single-molecule junctions with more reproducible current–voltage characteristics[19]. This allows us to extract average conductance values from thousands of individual measurements on a series of seven biphenyl molecules with different ring substitutions that alter the twist angle of the molecules. We find that the conductance for the series decreases with increasing twist angle, consistent with a cosine-squared relation predicted for transport through π-conjugated biphenyl systems[13].

We recently demonstrated that metal–molecule–metal junctions, formed by breaking Au point contacts in a solution of molecules, exhibit more reliable and reproducible conductance values when amine groups rather than thiols or isonitriles are used to attach the molecules to the junction contacts[19]. Because of this reduced variability, we can determine statistically meaningful average conductance values for specific single-molecule junctions; this capability in turn allows us to study the effect of molecular properties on junction conductance.

We present our experimental results as conductance histograms, where peaks indicate the most prevalent molecular junction conductances while the width of the conductance distributions reflects the microscopic variations from junction to junction. (For details of experimental and data analysis procedures, see Supplementary Information.) Figure 1a shows the histograms for 1,4-diaminobenzene (**1**) and 2,7-diaminofluorene (**2**), each constructed from thousands of conductance traces without resorting to any data selection or processing. All conductance traces reveal step-wise changes in conductance at conductance values that are close to multiples of the fundamental quantum of conductance, G_0 ($G_0 = 2e^2/h$, where e is the charge on an electron, and h is Planck's constant). In addition, many traces also exhibit step changes below G_0 that are due to conduction through a single molecule bridging the gap between the two Au point-contacts (see Fig. 1c and Supplementary Fig. S1). As seen in the histograms of **1** and **2** (Fig. 1a), for each junction type the

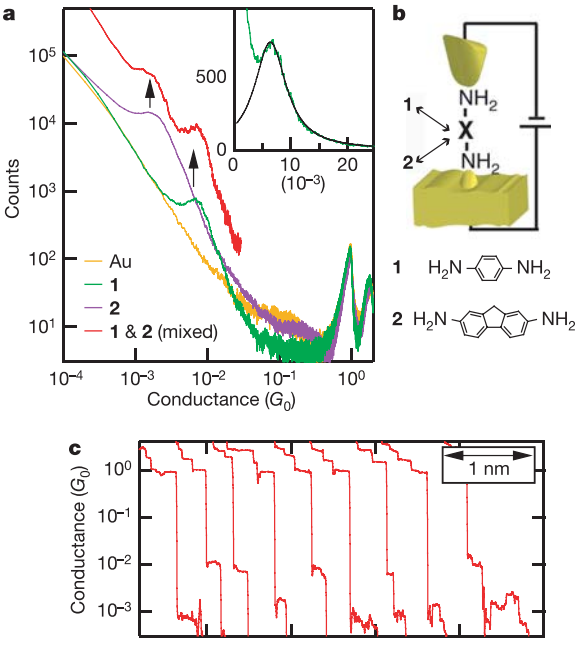

Figure 1 | Conductance measurements of 1,4-diaminobenzene and 2,7-diaminofluorene junctions. a, Conductance histogram of **1** (green; constructed from 10,000 traces and scaled by 1/10) and **2** (purple; constructed from 15,000 traces and scaled by 1/15) on a log–log scale, along with a control histogram of Au measured without molecules in the junction (yellow; constructed from 6,000 traces and scaled by 1/6). Peaks are clearly visible at G_0 and $2G_0$ for all three curves, and at $6.4 \times 10^{-3} G_0$ for **1** and at $1.5 \times 10^{-3} G_0$ for **2**. Also shown is a histogram collected for an equimolar solution of both molecules (vertically offset red curve; constructed from 4,000 traces and scaled by 1/4) showing two peaks indicated by the arrows corresponding to the individual peaks in the green and purple curve. Inset, lorentzian fit to the sub-G_0 peak in the histogram of **1**; note that conductance and counts are now shown on a linear scale. The bin size is $10^{-5} G_0$ for all histograms, and data were collected using a fixed bias voltage of 25 mV. **b**, Top, illustration of a gap between a gold point-contact and a gold surface that can be bridged with either molecule **1** or **2** from the surrounding solution. Bottom, structure of **1** and **2**. **c**, Sample conductance traces obtained when pulling the point contacts apart, and exhibiting step-wise changes corresponding to the conductance of molecule **1** and **2**.

[1]Department of Physics, [2]Department of Chemistry, [3]Department of Applied Physics and Applied Mathematics, and [4]Center for Electron Transport in Molecular Nanostructures, Columbia University, New York, USA.

additional step occurs within a narrow distribution of conductance values. The most prevalent value is determined by a fit to the peak below G_0 in the conductance histograms using a lorentzian line shape, which we find fits our peaks more accurately than a gaussian line shape (see Fig. 1a inset, and Supplementary Information).

When the experiment is repeated using a solution containing an equimolar mixture of **1** and **2** (as indicated in Fig. 1b), the resulting histogram (red curve in Fig. 1a) shows two distinct peaks below G_0 at nearly the same conductance values as those of the peaks seen in the histograms for the individual molecules (green and purple curves). Individual traces using the solution mixture show conductance plateaus corresponding to either molecule **1** or **2**, and sometimes a plateau corresponding to **1** followed by a plateau corresponding to **2** (Fig. 1c). But we do not see evidence of rapid fluctuations between the two, so the molecules are not exchanging position within the junction on the timescale of the experimental traces (few milliseconds for each trace). This provides further evidence that the conduction is through an individual molecule, not an ensemble.

Molecules **1** and **2** do not have an internal twist degree of freedom, but the two benzene rings of a biphenyl can rotate relative to one another. For such a molecule, as the twist angle (θ) between the two rings increases and simultaneously the degree of π-conjugation between them decreases, the junction conductance will decrease because molecular electron transfer rates scale as the square of the π-overlap[14,20]. When neglecting the contribution of tunnelling transport through the σ-orbitals (which is within the error of our measurements), then theory predicts a $\cos^2\theta$ relation[13]. We probe this relation between molecule twist angle and conductance using seven different biphenyl molecules (molecules **2** to **8** listed in Table 1), where the size of the substituents on the proximal carbons is optimized to create structures with a twist angle ranging from flat to essentially perpendicular. Figure 2a shows the structure of four (**2**, **4**, **6** and **8**) out of the seven molecules used. For each molecule, the average junction conductance is determined from the location of the peak in the conductance histogram, whereas the twist angle is determined theoretically for each molecule by assuming a fully relaxed and static geometry (see Table 1 and Supplementary Information; but effects of dynamic structural fluctuations of the molecule in the junction will also be discussed later on).

Figure 2b shows the measured conductance histograms for the molecules in Fig. 2a. For the flat molecule (**2**), the histogram peak yields an average junction conductance value of $1.5 \times 10^{-3} G_0$. For 4,4′-diaminobiphenyl (**4**) with equal molecular length but a twist angle θ of 34°, the conductance histogram shows a peak occurring at a lower conductance of $1.1 \times 10^{-3} G_0$. As the angle between the two aromatic rings is increased further to 52° in 4,4′-diaminooctafluorobiphenyl (**6**), the conductance value also drops further, to $4.9 \times 10^{-4} G_0$. When all four hydrogens on the proximal carbons of this molecule are replaced with methyls to give 2,6,2′,6′-tetramethyl-4,4′-diaminobiphenyl (**8**) with a twist angle θ of about 88°, most counts in the histogram occur for low junction conductance values. In Fig. 2c, we plot the peak conductance value measured for the seven molecules against $\cos^2\theta$ and fit the data with a $\cos^2\theta$ curve (dashed line in Fig. 2c). The good fit indicates that the electronic effects of the substituents do not significantly alter the simple picture that junction conductance may be adjusted by simply decreasing the π-overlap between phenyl rings within the bridging molecule.

Further evidence for tunnelling conductance through these aromatic diamine junctions is provided by Fig. 3a, which compares the histograms for a series of oligophenyls (molecules **1**, **4**, **9**) with 1, 2 and 3 phenyl rings. The inset shows that the plot of junction conductance versus molecule length fits an exponential form with a decay constant of 1.7 ± 0.1 per phenyl ring. This behaviour is direct evidence for non-resonant tunnelling transport through the

Table 1 | Molecular structure and measured properties

Molecule number	Structure	Conductance (G_0)		Peak width*	Twist angle (°)
		Measured	Calculated		
1	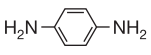	6.4×10^{-3}	6.4×10^{-3}	0.4	–
2	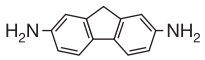	1.54×10^{-3}	2.1×10^{-3}	0.8	0
3	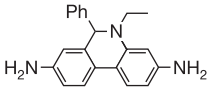	1.37×10^{-3}	2.2×10^{-3}	0.8	17
4	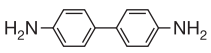	1.16×10^{-3}	1.6×10^{-3}	0.9	34
5	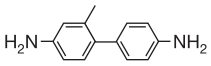	6.5×10^{-4}	1.2×10^{-3}	1.3	48
6	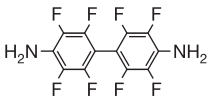	4.9×10^{-4}	7.1×10^{-4}	0.6	52
7	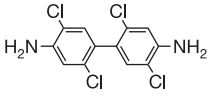	3.7×10^{-4}	5.8×10^{-4}	0.9	62
8	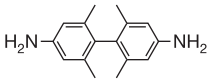	7.6×10^{-5}†	6.4×10^{-5}	NA†	88
9	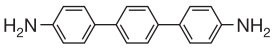	1.8×10^{-4}‡	3.5×10^{-4}	2.1	–

Table shows molecule structure, measured conductances, calculated relative conductances, relative widths of the histogram peaks (see Supplementary Information for details) and the calculated twist angle, θ.

*Half-width at half-maximum of the lorentzian fit, normalized to the peak value.

†The histogram peak was determined after subtracting the Au histogram from the data, as the raw data could not be fitted with a lorentzian so a width could not be determined.

‡Determined from actual maximum of the raw data.

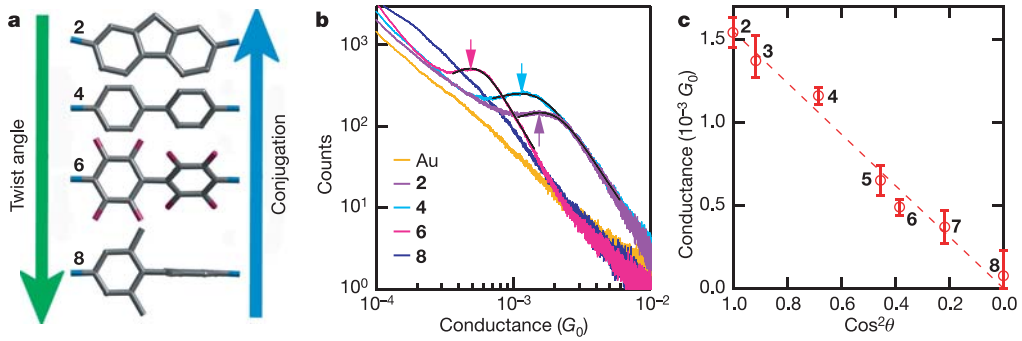

Figure 2 | Biphenyl junction conductance as a function of molecular twist angle. **a**, Structures of a subset of the biphenyl series studied, shown in order of increasing twist angle or decreasing conjugation. **b**, Conductance histograms obtained from measurements using molecule **2** (purple; constructed from 15,000 traces and scaled by 1/15), **4** (cyan; constructed from 7,000 traces and scaled by 1/7), **6** (pink; constructed from 11,000 traces and scaled by 1/11) and **8** (blue; constructed from 5,000 traces and scaled by 1/5). Also shown is the control histogram obtained from measurements without molecules between the contacts (yellow; constructed from 6,000 traces and scaled by 1/6). Arrows point to the peak conductance values obtained from lorentzian fits (solid black curves). All data were taken at a bias voltage of 25 mV. **c**, Position of the peaks for all the molecules studied plotted against $\cos^2\theta$, where θ, the calculated twist angle for each molecule, is listed in Table 1. Error bars are determined from the standard deviation of the peak locations determined from the fits to histograms of 1,000 traces (see Supplementary Information.)

amine-terminated molecules[14,20–24], with the measured decay constant being close to the estimate of 1.5 per phenyl ring that we obtain[25–27] for these molecules (see Supplementary Information). In Table 1, we also compare the measured conductance of all molecules with an estimated relative conductance, obtained by calculating the square of the tunnel coupling of each molecule and normalizing this value to the measured conductance of molecule **1**. This comparison indicates that the trend in the measured conductances is largely accounted for by the change in tunnelling with molecular conformation.

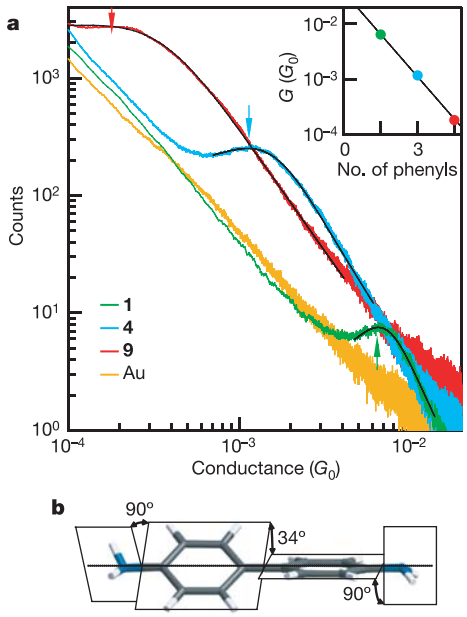

Figure 3 | Polyphenyl junction conductance as a function of the number of phenyl units. **a**, Conductance histograms for molecular junctions of **1** (green; constructed from 10,000 traces and scaled by 1/10), **4** (cyan; constructed from 7,000 traces and scaled by 1/7), and **9** (red; constructed from 3,000 traces and scaled by 1/3), along with a control histogram obtained from measurements without molecules between the contacts (yellow; constructed from 6,000 traces and scaled by 1/6). Bin size is $10^{-5}G_0$ for the green trace (and is therefore offset vertically by a factor of 10) and $10^{-6}G_0$ for the other traces. Arrows point to the peaks. Lorentzian fits (solid black curves) are also shown. All data were taken at 25 mV bias voltage. Inset, peak conductance values obtained with **1**, **4** and **9** versus the molecules' number of phenyl rings, on a semi-log scale. The black line shows an exponential fit to the data points. **b**, Illustration of molecule **4**, highlighting the three twist angles that influence conductance through the metal–molecule–metal junction, and which are defined as the angles between the adjacent planes shown in the figure. In solution, molecule **4** has a thermally averaged conformation with a ring–ring twist angle and amine–ring twist angles close to the potential minimum values of 34° and 90°, respectively.

The results presented so far agree quite well with predictions of non-resonant tunnelling transport through static molecules. However, it is well established that the energy barriers for ring rotations in unsubstituted biphenyls such as **4** are about 0.1 eV or 2–3 kcal mol^{-1} (ref. 28; the barriers are altered by the substituents in the molecules **5**–**8**, and are substantially higher (Supplementary Information)). Therefore at room temperature, such molecules in the junction can be expected to fully explore low-energy rotations. The measurement times are long compared to the rate of molecular rotations in solution (each conductance step lasts a few milliseconds), so the conductance level measured at each step on a single trace is a thermal average over any fast dynamic fluctuations. But even though the rotation barrier is small for molecule **4**, our calculations indicate that thermal averaging still results in a conductance value that is close to the value characteristic of a static molecule in its lowest energy conformation.

The data in Figs 1–3 also reveal another interesting trend: as the molecule is granted additional rotational degrees of freedom, the conductance peak broadens. This is in contrast to the data for the diamino-alkane series[19], where the histogram peak widths are similar for all molecules and are associated only with the modest variations in the electronic coupling through the Au–amine link. The peak broadening for the aromatics (widths in Table 1) is most clearly seen in Fig. 3a for the oligophenyl series. The sharpest peak is observed for **1**, while the peaks in the histograms are systematically broader for biphenyl- and terphenyl-diamines (**4** and **9**), where the individual phenyl rings can rotate about the σ-bond that connects them. Individual conductance traces show steps (Supplementary Figs S1 and S2) that occur over an expanded the range. We therefore suggest that in each junction formed during the measurements, the molecule is in a different average conformation enabled by its rotational degrees of freedom and that each different conformation has a different characteristic conductance. In solution, the thermally averaged conformation for molecule **4** would have both the ring–ring twist angle and the two amine–ring twist angles close to their rotational barrier minima of 34° and 90° respectively (angles illustrated in Fig. 3b). Upon junction formation, each Au–N link is pinned by the particular Au–N bonding environment. This provides a mechanism to skew the twist angles of the trapped molecule. The average twist angles of the three rotatable bonds in the trapped molecule (the C–C and the two C–N σ-bonds) would then differ from those in the unbound molecule, with the bond that has a lower

energy barrier for rotation accommodating a larger change. This results in wider histograms, although the histogram peaks, which correspond to the most probable Au–molecule–Au conformations, are still located close to the lowest energy conformation.

Received 27 March; accepted 23 June 2006.

1. Aviram, A. & Ratner, M. Molecular rectifiers. *Chem. Phys. Lett.* **29,** 277–283 (1974).
2. Reed, M. A., Zhou, C., Muller, C. J., Burgin, T. P. & Tour, J. M. Conductance of a molecular junction. *Science* **278,** 252–254 (1997).
3. Porath, D., Bezryadin, A., de Vries, S. & Dekker, C. Direct measurement of electrical transport through DNA molecules. *Nature* **403,** 635–638 (2000).
4. Cui, X. D. *et al.* Reproducible measurement of single-molecule conductivity. *Science* **294,** 571–574 (2001).
5. Reichert, J. *et al.* Driving current through single organic molecules. *Phys. Rev. Lett.* **88,** 176804 (2002).
6. Xu, B. Q. & Tao, N. J. J. Measurement of single-molecule resistance by repeated formation of molecular junctions. *Science* **301,** 1221–1223 (2003).
7. Dadosh, T. *et al.* Measurement of the conductance of single conjugated molecules. *Nature* **436,** 677–680 (2005).
8. Park, J. *et al.* Coulomb blockade and the Kondo effect in single-atom transistors. *Nature* **417,** 722–725 (2002).
9. Liang, W. J., Shores, M. P., Bockrath, M., Long, J. R. & Park, H. Kondo resonance in a single-molecule transistor. *Nature* **417,** 725–729 (2002).
10. Nazin, G. V., Qiu, X. H. & Ho, W. Visualization and spectroscopy of a metal–molecule–metal bridge. *Science* **302,** 77–81 (2003).
11. Guisinger, N. P., Yoder, N. L. & Hersam, M. C. Probing charge transport at the single-molecule level on silicon by using cryogenic ultra-high vacuum scanning tunneling microscopy. *Proc. Natl. Acad. Sci. USA* **102,** 8838–8843 (2005).
12. Piva, P. G. *et al.* Field regulation of single-molecule conductivity by a charged surface atom. *Nature* **435,** 658–661 (2005).
13. Woitellier, S., Launay, J. P. & Joachim, C. The possibility of molecular switching: Theoretical study of $[(NH_3)_5Ru\text{-}4,4'\text{-}Bipy\text{-}Ru(NH_3)_5]^{5+}$. *Chem. Phys.* **131,** 481–488 (1989).
14. Mujica, V. *et al.* Electron transfer in molecules and molecular wires: Geometry dependence, coherent transfer, and control. *Adv. Chem. Phys.* **107,** 403–429 (1999).
15. Moresco, F. *et al.* Conformational changes of single molecules induced by scanning tunneling microscopy manipulation: A route to molecular switching. *Phys. Rev. Lett.* **86,** 672–675 (2001).
16. Dulic, D. *et al.* One-way optoelectronic switching of photochromic molecules on gold. *Phys. Rev. Lett.* **91,** 207402 (2003).
17. Yasuda, S., Nakamura, T., Matsumoto, M. & Shigekawa, H. Phase switching of a single isomeric molecule and associated characteristic rectification. *J. Am. Chem. Soc.* **125,** 16430–16433 (2003).
18. Oliver, A. M., Craig, D. C., Paddonrow, M. N., Kroon, J. & Verhoeven, J. W. Strong effects of the bridge configuration on photoinduced charge separation in rigidly linked donor–acceptor systems. *Chem. Phys. Lett.* **150,** 366–373 (1988).
19. Venkataraman, L. *et al.* Single-molecule circuits with well-defined molecular conductance. *Nano Lett.* **6,** 458–462 (2006).
20. Nitzan, A. Electron transmission through molecules and molecular interfaces. *Annu. Rev. Phys. Chem.* **52,** 681–750 (2001).
21. Wold, D. J., Haag, R., Rampi, M. A. & Frisbie, C. D. Distance dependence of electron tunneling through self-assembled monolayers measured by conducting probe atomic force microscopy: Unsaturated versus saturated molecular junctions. *J. Phys. Chem. B* **106,** 2813–2816 (2002).
22. Tomfohr, J. K. & Sankey, O. F. Complex band structure, decay lengths, and Fermi level alignment in simple molecular electronic systems. *Phys. Rev. B* **65,** 245105 (2002).
23. Ratner, M. A. *et al.* Molecular wires: Charge transport, mechanisms, and control. Molecular electronics. *Sci. Technol.* **852,** 22–37 (1998).
24. Launay, J. P. Long-distance intervalence electron transfer. *Chem. Soc. Rev.* **30,** 386–397 (2001).
25. Perdew, J. P., Burke, K. & Ernzerhof, M. Generalized gradient approximation made simple. *Phys. Rev. Lett.* **77,** 3865–3868 (1996).
26. Jaguar Version 5 Release 19 (Schrodinger, Portland, Oregon, 2002).
27. Wadt, W. R. & Hay, P. J. *Ab initio* effective core potentials for molecular calculations–Potentials for main group elements Na to Bi. *J. Chem. Phys.* **82,** 284–298 (1985).
28. Almenningen, A. *et al.* Structure and barrier of internal rotation of biphenyl derivatives in the gaseous state: Part 1. The molecular structure and normal coordinate analysis of normal biphenyl and perdeuterated biphenyl. *J. Mol. Struct.* **128,** 59–76 (1985).

Supplementary Information is linked to the online version of the paper at www.nature.com/nature.

Acknowledgements We thank H. Stormer, P. Kim and J. Fernandez for discussions. This research was supported by the NSF Nanoscale Science and Engineering Center at Columbia University, New York State Office of Science (NYSTAR). C.N. thanks the Camille Dreyfus Teacher Scholar Program (2004) and the Alfred P. Sloan Fellowship Program (2004); J.E.K. thanks the American Chemical Society Division of Organic Chemistry for the graduate fellowship sponsored by Organic Syntheses; and M.L.S. thanks the Material Research Science and Engineering Center Program of the NSF.

Author Information Reprints and permissions information is available at www.nature.com/reprints. The authors declare no competing financial interests. Correspondence and requests for materials should be addressed L.V. (latha@phys.columbia.edu) or M.S.H (msh2102@columbia.edu).